

We are IntechOpen, the world's leading publisher of Open Access books Built by scientists, for scientists

6,900

Open access books available

186,000

International authors and editors

200M

Downloads

Our authors are among the

154

Countries delivered to

TOP 1%

most cited scientists

12.2%

Contributors from top 500 universities



WEB OF SCIENCE™

Selection of our books indexed in the Book Citation Index
in Web of Science™ Core Collection (BKCI)

Interested in publishing with us?
Contact book.department@intechopen.com

Numbers displayed above are based on latest data collected.
For more information visit www.intechopen.com



Traveling Wave Solutions and Chaotic Motions for a Perturbed Nonlinear Schrödinger Equation with Power-Law Nonlinearity and Higher-Order Dispersions

*Mati Youssoufa, Ousmanou Dafounansou,
Camus Gaston Latchio Tiofack and Alidou Mohamadou*

Abstract

This chapter aims to study and solve the perturbed nonlinear Schrödinger (NLS) equation with the power-law nonlinearity in a nano-optical fiber, based upon different methods such as the auxiliary equation method, the Stuart and DiPrima's stability analysis method, and the bifurcation theory. The existence of the traveling wave solutions is discussed, and their stability properties are investigated through the modulational stability gain spectra. Moreover, the development of the chaotic motions for the systems is pointed out *via* the bifurcation theory. Taking into account an external periodic perturbation, we have analyzed the chaotic behavior of traveling waves through quasiperiodic route to chaos.

Keywords: nano-optical fibers, perturbed nonlinear Schrödinger equation, auxiliary equation method, exact traveling wave solutions, modulational instability, planar dynamic system, chaotic motions

1. Introduction

The wave process is innumerable in nature. Such familiar examples include water waves, plasma waves, and optical waves and are governed by nonlinear partial differential equations. The study of nonlinear evolution equations helps a lot in understanding certain interesting physical properties posed by themselves, in several physical systems. Recently, an important amount of studies has been related to nonlinear systems having multidegrees of freedom: The well-known nonlinear Schrödinger (NLS) equation is a particular example. The idea behind the NLS equation was originated from the work of Erwin Schrödinger, an Autrichian physician, in 1926 [1]. This equation governs weakly nonlinear and dispersive wave packets in one-dimensional (1D) physical systems. It was first derived, in a general setting, by Benney and Newell in 1967 [2]. Also, it was derived in the study of modulational stability of deep-water waves by Zakharov in 1968 [3]. Afterward, Hasegawa and Tappert (1973) showed that the same equation governs light-pulse

propagation in optical fibers [4]. For instance, the cubic-NLS has been widely used to model the propagation of light pulse in material's systems involving third-order susceptibility $\chi^{(3)}$ [5–7]. In the same context, the nonlinear interaction between the high-frequency Langmuir waves and the ion-acoustic waves by ponderomotive forces [8, 9] in a region of reduced plasma density, and the nonlinear interaction between Langmuir waves and electrons, were described by the “*parabolic law nonlinearity*” (cubic-quintic CQ) that existing in nonlinear media such as the $\text{CdS}_x\text{Se}_{1-x}$ –doped glass [10, 11], the poly-toluene sulfonate (PTS) crystals, special semiconductor waveguides (e.g., AlGaAs, CdS) [12]. Furthermore, Serkin et al. [13], Dai et al. [14], and others have devoted pioneering works in order to analyze the dynamical propagation of light pulse in CQ-nonlinear media, by considering the CQ-NLS equation.

Generally, the NLS-type models are important classes of nonlinear evolution equations that play a crucial role in the study of nonlinear dynamical problems in several areas of nonlinear sciences such as nonlinear optics, plasmas and Bose-Einstein condensates, and nano-optical fibers among others [15–18]. Although these equations explain the pulse dynamics in optical fibers [19–22], some of these nonlinear models are non-integrable. In this context, various computational and analytical methods have been proposed and used in the past few decades, to examine many classes of Schrödinger equation [23–42]. Nonetheless, these investigations reveal that the dynamic of solutions in non-integrable systems can be important and more complex.

Our study will be focused on a nano-optical fiber-system, described by the following extended perturbed NLS equation (integrable equation named as Biswas-Arshed model), involving power-law nonlinearity and higher-order dispersions [20–22]:

$$i\psi_z + a_1\psi_{xx} + a_2\psi_{xt} + b_1|\psi|^{2n}\psi + b_2|\psi|^{4n}\psi - i\left[\alpha\psi_x + \gamma(|\psi|^{2n}\psi)_x + \sigma(|\psi|^{2n})_x\psi + \delta(|\psi|^{4n}\psi)_x + \lambda(|\psi|^{4n})_x\psi + \theta|\psi|^{2n}\psi_x\right] = 0, \quad (1)$$

where the complex-valued function $\psi(z, x)$ is designated for waveform, which depends on the temporal variable z and the spatial variable x ; a_1 and a_2 are, respectively, the group velocity dispersion (GVD) and spatiotemporal dispersion coefficients (STD). b_1 and b_2 correspond to the coefficient of power-law nonlinearity; α accounts for the inter-modal dispersion. γ and δ account for the self-steepening perturbation terms, while σ , λ , and θ provide the effect of nonlinear dispersion coefficient. Finally, n denotes the strength of the power-law nonlinearity.

This model is relevant to some applications in which higher-order nonlinearities are important and describe the dynamics of solitary-wave propagation through optical fibers and other forms of waveguides, and contains, under different circumstances, several integrable NLS-types such as the Hirota equation [43], the Sasa Satsuma model [44], Gerdjikov-Ivanov equation, Lakshmanan-Porsezian-Daniel model, Schrödinger-Hirota equation, and a variety of other such models. More specially, Eq. (1) with $b_2 = \sigma = \delta = \lambda = \theta = 0$ and $0 < n < 2$ was used to study chaotic motions for the perturbed NLS equation with the power-law nonlinearity based on the equilibrium points by Yin et al. [20] and was also considered by Savescu et al. [45] to analyze nonlinear dynamical problems in the nano-optical fibers. Here, we study the model Eq. (1) with arbitrary parameters that are valid for several types of highly nonlinear mediums and give rise to some new results. For this purpose, we would like to obtain the exact solutions of Eq. (1) by using the auxiliary equation method [46–48] and the bifurcation theory of planar dynamical systems [49, 50].

The auxiliary equation method is a powerful solution method for the computation of exact traveling wave and soliton solutions. It is one of the most direct and effective algebraic methods for finding exact solutions of nonlinear partial differential equations. This method is applicable to a large class of equations and does not need therefore to make strong assumptions about the nonlinear equations, as compared to the well-known inverse scattering transform, which uses powerful analytical methods and therefore makes strong assumptions.

The bifurcation theory of planar dynamical systems plays a crucial role in the study of the evolution of higher-order nonlinear equations. The bifurcation analysis can be used to obtain chaotic motions for Eq. (1) based on the equilibrium points.

We will discuss model Eq. (1) and explore the dynamics of traveling wave solutions by employing the auxiliary equation method. In addition, using the linear stability analysis formulation, we will analyze and report the typical outcomes of the nonlinear development of the modulational instability (MI). Finally, we will point out the development of the chaotic motions for systems described by Eq. (1) through the bifurcation theory.

2. Exact solutions

2.1 The auxiliary equation method

In order to obtain the exact analytic traveling wave solutions of Eq. (1), we can employ the auxiliary equation method by considering the following transformation:

$$\psi(z, x) = U(\zeta)e^{i\phi(\zeta)}, \quad \zeta = k_1x - k_2z. \quad (2)$$

Here, k_1 and k_2 are real constants, $U(\zeta)$ denotes the amplitude and $\phi(\zeta)$ characterizes the phase component of the soliton.

Putting Eq. (2) into Eq. (1) and separating the real and imaginary parts, one obtains

$$\begin{aligned} & b_1U^{2n+1} + (b_2 + k_1\phi_\zeta)U^{4n+1} + k_1(\gamma + \theta)\phi_\zeta U^{2n+1} + (k_2 + \alpha k_1)\phi_\zeta U \\ & - k_1(a_1k_1 - a_2k_2)(\phi_\zeta^2 U + U_{\zeta\zeta}) = 0, \end{aligned} \quad (3)$$

and

$$\begin{aligned} & -k_1[\delta + 4n(\delta + \lambda)]U_\zeta U^{4n} - (k_2 + \alpha k_1)U_\zeta - k_1[\gamma + \theta + 2n(\gamma + \sigma)]U_\zeta U^{2n} \\ & + k_1(a_1k_1 - a_2k_2)(2\phi_\zeta U_\zeta + \phi_{\zeta\zeta} U) = 0. \end{aligned} \quad (4)$$

We set:

$$\phi_\zeta = p_1 - p_2 U^{2n}, \quad \phi_{\zeta\zeta} = -2np_2 U_\zeta U^{2n-1}. \quad (5)$$

The substitution of Eq. (5) into Eq. (4) gives

$$p_1 = \frac{k_2 + \alpha k_1}{2k_1(a_1k_1 - a_2k_2)}, \quad p_2 = -\frac{\gamma + \theta + 2n(\gamma + \sigma)}{2(n+1)(a_1k_1 - a_2k_2)}, \quad (6)$$

under the restraint relation

$$\lambda = -(4n+1)\delta. \quad (7)$$

Plugging Eq. (5) into Eq. (3) with respect to Eqs. (6) and (7), we get

$$\begin{aligned} & k_1(a_1k_1 - a_2k_2)U_{\zeta\zeta} + [p_1(k_2 + \alpha k_1) - p_1^2k_1(a_1k_1 - a_2k_2)]U \\ & + [b_1 + k_1p_1(\gamma + \theta) + p_2(k_2 + \alpha k_1) - 2p_1p_2k_1(a_1k_1 - a_2k_2)]U^{2n+1} \\ & + [b_2 + k_1p_1 + k_1p_2(\gamma + \theta) - p_2^2k_1(a_1k_1 - a_2k_2)]U^{4n+1} + k_1p_2U^{6n+1} = 0. \end{aligned} \quad (8)$$

The substitution of

$$U(\zeta) = V^{\frac{1}{2n}}(\zeta), \quad (9)$$

in Eq. (8) yields:

$$\begin{aligned} & k_1(a_1k_1 - a_2k_2) \left[2nVV_{\zeta\zeta} + (1 - 2n)(V_{\zeta})^2 \right] + 4n^2k_1p_2V^5 \\ & + 4n^2[b_2 + k_1p_1 + k_1p_2(\gamma + \theta) - p_2^2k_1(a_1k_1 - a_2k_2)]V^4 \\ & + 4n^2[b_1 + k_1p_1(\gamma + \theta) + p_2(k_2 + \alpha k_1) - 2p_1p_2k_1(a_1k_1 - a_2k_2)]V^3 \\ & + 4n^2[p_1(k_2 + \alpha k_1) - p_1^2k_1(a_1k_1 - a_2k_2)]V^2 = 0. \end{aligned} \quad (10)$$

We consider the trial equation as [46, 47]:

$$(V_{\zeta})^2 = F(V) = \sum_{l=0}^N \mu_l V^l, \quad (11)$$

where $\mu_l (l = 0, 1, \dots, N)$ are constants to be determined according to the balance principle. The previous Eq. (11) can be rewritten by the integral form

$$\pm(\zeta - \zeta_0) = \int \frac{dV}{\sqrt{F(V)}}. \quad (12)$$

Balancing $VV_{\zeta\zeta}$ and V^5 in Eq. (10), we get $N = 5$. Using the solution procedure of the trial equation method [46, 47], a system of algebraic equations is obtained (see Appendix) and the resolution of this obtained system yields the following:

$$\begin{aligned} \mu_0 &= 0, \mu_1 = 0, \mu_2 = 4n^2 \left[p_1^2 - \frac{p_1(k_2 + \alpha k_1)}{k_1(a_1k_1 - a_2k_2)} \right], \\ \mu_3 &= \frac{4n^2}{n+1} \left[2p_1p_2 - \frac{b_1 + k_1p_1(\gamma + \theta) + p_2(k_2 + \alpha k_1)}{k_1(a_1k_1 - a_2k_2)} \right], \\ \mu_4 &= \frac{4n^2}{2n+1} \left[p_2^2 - \frac{b_2 + k_1p_1 + k_1p_2(\gamma + \theta)}{k_1(a_1k_1 - a_2k_2)} \right], \\ \mu_5 &= -\frac{4n^2p_2}{(a_1k_1 - a_2k_2)(3n+1)}. \end{aligned} \quad (13)$$

Now, from Eqs. (11) and (12), we can write

$$\pm(\zeta - \zeta_0) = \int \frac{dV}{V \sqrt{\mu_2 + \mu_3 V + \mu_4 V^2 + \mu_5 V^3}}. \quad (14)$$

The integral Eq. (14) admits many types of solutions that can be listed in accordance with [51–53].

Since $\mu_2 = 4n^2 \left[p_1^2 - \frac{p_1(k_2 + \alpha k_1)}{k_1(a_1 k_1 - a_2 k_2)} \right] = -\frac{n^2(k_2 + \alpha k_1)^2}{k_1^2(a_1 k_1 - a_2 k_2)^2} < 0$, and in order to highlight our analysis, we consider the following parametric setting $\gamma = -\sigma = -\theta$. After these considerations, the phase component of the soliton can be written as follows:

$$\phi(z, x) = \frac{k_2 + \alpha k_1}{2k_1(a_1 k_1 - a_2 k_2)}(k_1 x - k_2 z) + c, \quad (15)$$

where c is a real constant number.

a. If $4\mu_2\mu_4 - \mu_3^2 = 0$ and $\mu_4 > 0$, we have the following exact traveling solution.

$$\psi_a(z, x) = \left\{ \frac{\mu_3}{4\mu_4} \left[1 \pm \cotanh \left(\frac{\mu_3 \sqrt{\mu_4}}{4\mu_4} (k_1 x - k_2 z) \right) \right] \right\}^{\frac{1}{2n}} e^{i\phi(z, x)}, \quad (16)$$

under the constraint $\mu_4 > 0$.

b. If $\mu_3^2 - 4\mu_2\mu_4 > 0$ and $\mu_2 < 0$ we get a singular periodic solution

$$\psi_b(z, x) = \left\{ \frac{2\mu_2}{-\mu_3 \pm \sqrt{\mu_3^2 - 4\mu_2\mu_4} \sin [\sqrt{-\mu_2}(k_1 x - k_2 z)]} \right\}^{\frac{1}{2n}} e^{i\phi(z, x)}. \quad (17)$$

2.2 Stability analysis method: Modulational instability (MI) of the continuous wave (CW) background

Modulational instability (MI) is a fundamental and ubiquitous phenomenon originating from the interplay between nonlinear self-interaction of wave fields and linear dispersion or diffraction. This process appears in most nonlinear systems [42, 52–57]. Unlike the well-known pulse kinds, the solitons are relatively stable, even in a perturbed environment.

In this section, we investigate the stability of the previous solutions that are sitting on a CW background, which may be subject to MI. To do so, we apply the standard linear stability analysis [52, 53, 56] on a generic CW (steady-state solution)

$$\psi_0(z, x) = P_0 e^{i(c_1 x + c_2 z)}, \quad (18)$$

where P_0 , c_1 , and c_2 are real constants.

Putting Eq. (18) into Eq. (1), we get:

$$c_2 = \frac{1}{1 + a_2 c_1} \{ (\alpha - a_1 c_1) c_1 + [b_1 + (\gamma + \theta) c_1] P_0^{2n} + (b_2 + \delta c_1) P_0^{4n} \}. \quad (19)$$

Adding infinitesimal perturbation field v on CW solutions by introducing the following expansion

$$\tilde{\psi}(z, x) = [P_0 + v(z, x)] e^{i(c_1 x + c_2 z)}, \quad (20)$$

one can find the linearized equation satisfied by the complex perturbation v as:

$$ir_1v_z + ir_2v_x + a_1v_{xx} + a_1v_{xz} + r_3(v + v^*) + ir_4(v_x + v_x^*) = 0, \quad (21)$$

where

$$\begin{aligned} r_1 &= 1 + a_2c_1, \\ r_2 &= 2a_1c_1 + a_2c_2 - \alpha - (\gamma + \theta)P_0^{2n} - \delta P_0^{4n}, \\ r_3 &= nP_0^{2n} [b_1 + (\gamma + \theta)c_1 + 2(b_2 + \delta c_1)P_0^{2n}], \\ r_4 &= -nP_0^{2n} [\gamma + \sigma + 2(\delta + \lambda)P_0^{2n}]. \end{aligned} \quad (22)$$

The solution of Eq. (21) is given by collecting the Fourier modes as

$$v(z, x) = v_+ e^{i(Kz - \Omega x)} + v_- e^{-i(Kz - \Omega x)}, \quad (23)$$

where Ω accounts for the wavenumber and K represents the frequency of perturbation. v_+ and v_- are much less than the background amplitude P_0 ($|v(z, x)| \ll P_0$). In this case, the instability of the steady state (CW) is achieved by the exponential growth of the perturbed field.

Deputing the expression of perturbed nonlinear background Eq. (23) into Eq. (21), we obtain after linearization, a system of homogeneous equations satisfied by v_+ and v_- :

$$\begin{pmatrix} (a_2\Omega - r_1)K + (r_2 + r_4)\Omega + r_3 - a_1\Omega^2 & r_3 + \Omega r_4 \\ r_3 - \Omega r_4 & (a_2\Omega + r_1)K - (r_2 + r_4)\Omega + r_3 - a_1\Omega^2 \end{pmatrix} \begin{pmatrix} v_+ \\ v_- \end{pmatrix} = \begin{pmatrix} 0 \\ 0 \end{pmatrix}. \quad (24)$$

This set has a nontrivial solution only when the previous 2×2 determinant matrix vanishes. By requiring the determinant of the associated matrix to be zero, we get the dispersion relation:

$$\begin{aligned} (a_2^2\Omega^2 - r_1^2)K^2 + 2\Omega[a_2(r_3 - a_1\Omega^2) + r_1(r_2 + r_4)]K + (r_3 - a_1\Omega^2)^2 \\ - \Omega^2(r_2 + r_4)^2 = 0. \end{aligned} \quad (25)$$

In order to observe MI, one of the two roots of the previous dispersion relation should possess a negative imaginary part, which corresponds to an exponential growth of the perturbation amplitude. So, the MI is measured by power gain, and it is defined at any pump frequency as [52, 53]:

$$g(\Omega) = 2|Im(K_{max})|, \quad (26)$$

where the factor 2 converts $g(\Omega)$ to power gain, and $Im(K_{max})$ denotes the imaginary part of the polynomial root with the largest value K_{max} .

Figure 1 depicts the MI gain spectra as a function of the modulation frequency (Ω) and second-order dispersion (a_1), for a fixed value of the initial power ($P_0 = 10kW$), the other parameter values being $a_2 = 0.005$, $b_1 = b_2 = \alpha = 0.2$, $c_1 = 2$, $\gamma = -\theta = -\sigma = 1$, $\delta = 0.5$. Firstly, we consider the strength of the power-law nonlinearity $n = 1$, which yields to symmetrical sidelobes of instability around the zero-perturbation frequency $\Omega = 0$ in **Figure 1(a)**. In this map, the width and magnitude of the two sidelobes remain constant in the normal group velocity dispersion ($a_1 < 0$), while they increase in the anomalous dispersion regime ($a_1 > 0$). For the nonlinearity power index $n = 2$, we obtain in **Figure 1(b)**, two similar sidelobes due to MI, which stand symmetrically around the line $\Omega = 0$. In this case,

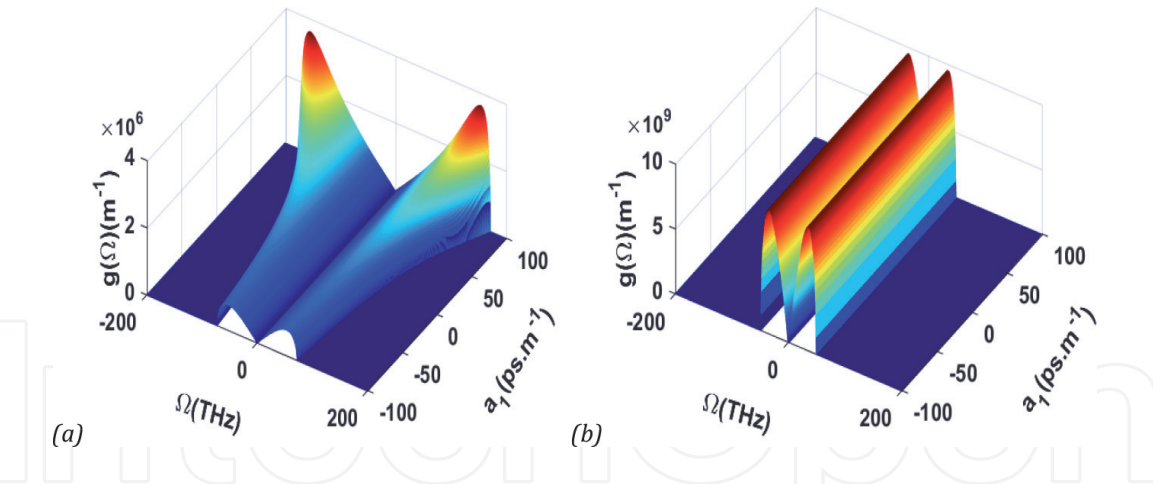


Figure 1. MI gain spectra $g(\Omega)$ versus frequency shift Ω and second-order dispersion a_1 for parameter values: $a_2 = 0.005$, $b_1 = b_2 = \alpha = 0.2$, $c_1 = 2$, $\gamma = -\theta = -\sigma = 1$, $\delta = 0.5$, $P_o = 10$: (a) $n = 1$; (b) $n = 2$.

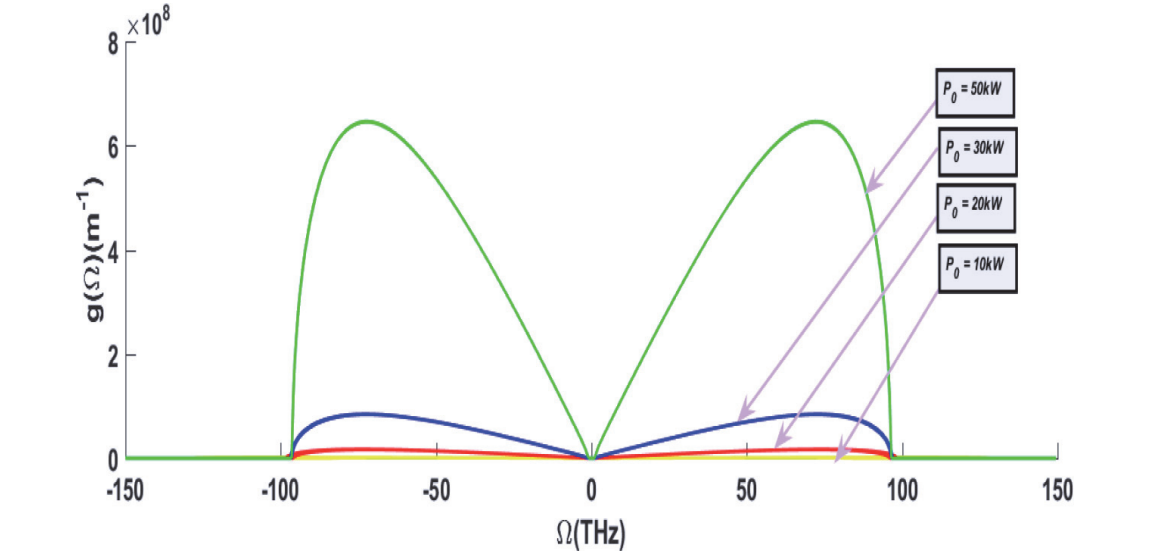


Figure 2. 2D plot showing the variation of the MI gain spectra $g(\Omega)$ versus frequency Ω at a four-power level P_o [for yellow solid line ($P_o = 10kW$), red solid line ($P_o = 20kW$), blue solid line ($P_o = 30kW$), and green solid line ($P_o = 50kW$)], with the same parameter values as in **Figure 1**.

the magnitude and width of the sidelobes remain constant in the normal as well as the anomalous dispersion regimes.

Figure 2 exhibits the enlarged MI gain spectra in 2D-plot at four power levels ($P_o = 10kW$; $20kW$; $30kW$; $50kW$) with the same values of parameters as in **Figure 1**. The MI gain profile, indicated by colored solid curves, is constitutive of two gain bands in the Stokes frequency shift region ($\Omega < 0$) and in the anti-Stokes frequency shift region ($\Omega > 0$). We can see that the MI gain exists only within a limited range of frequency ($|\Omega| < 100$) and the maximum gain increases with the increasing input power P_o .

3. Planar dynamical system and Hamiltonian: Phase portraits

In this section, we transform Eq. (8) to a dynamical system by introducing new variables X and Y , in order to investigate the equilibrium points, the periodic, quasiperiodic, and chaotic motions of systems in the presence of an external periodic perturbation, *via* the bifurcation method [49, 50, 58].

3.1 Formation of a dynamical system

Now, we rewrite Eq. (8) as

$$U_{\zeta\zeta} = AU + BU^{2n+1} + CU^{4n+1} + DU^{6n+1}, \quad (27)$$

where

$$\begin{aligned} A &= p_1^2 - \frac{p_1(k_2 + \alpha k_1)}{k_1(a_1 k_1 - a_2 k_2)} = -\frac{(k_2 + \alpha k_1)^2}{4k_1^2(a_1 k_1 - a_2 k_2)^2} < 0, \\ B &= 2p_1 p_2 - \frac{b_1 + k_1 p_1(\gamma + \theta) + p_2(k_2 + \alpha k_1)}{k_1(a_1 k_1 - a_2 k_2)}, \\ C &= p_2^2 - \frac{b_2 + k_1 p_1 + k_1 p_2(\gamma + \theta)}{k_1(a_1 k_1 - a_2 k_2)}, \\ D &= -\frac{k_1 p_2}{k_1(a_1 k_1 - a_2 k_2)}. \end{aligned} \quad (28)$$

By setting

$$X = U, Y = U_\zeta, \quad (29)$$

we can rewrite Eq. (27) as a planar dynamical system

$$\begin{cases} X_\zeta = Y, \\ Y_\zeta = f(X) = AX + BX^{2n+1} + CX^{4n+1} + DX^{6n+1}. \end{cases} \quad (30)$$

The Hamiltonian of the dynamical system Eq. (30) is defined as

$$H(X, Y) = \frac{1}{2}Y^2 - \frac{A}{2}X^2 - \frac{B}{2(n+1)}X^{2n+2} - \frac{C}{2(2n+1)}X^{4n+2} - \frac{D}{2(3n+1)}X^{6n+2}, \quad (31)$$

and satisfy to

$$\frac{dH}{d\zeta} = \frac{\partial H}{\partial \zeta} X_\zeta + \frac{\partial H}{\partial X} Y_\zeta = 0. \quad (32)$$

This result implies that the Hamiltonian is a constant of motion [i.e., $H(X, Y) \equiv Cst$] and the system Eq. (30) is an integrable Hamiltonian system.

3.2 Chaotic motion analysis

3.2.1 Equilibrium state derivation

Using the bifurcation analysis and qualitative theory, we analyze equilibrium points for system Eq. (30). We consider the following Jacobian matrix of system (30) at the equilibrium points (X_k, Y_k) :

$$J = \begin{pmatrix} \frac{\partial X_\zeta}{\partial X} & \frac{\partial X_\zeta}{\partial Y} \\ \frac{\partial Y_\zeta}{\partial X} & \frac{\partial Y_\zeta}{\partial Y} \end{pmatrix} = \begin{pmatrix} 0 & 1 \\ A + (2n+1)BX_k^{2n} + (4n+1)CX_k^{4n} + (6n+1)DX_k^{6n} & 0 \end{pmatrix}, \quad (33)$$

where X_k are the zeros (solutions) of $f(X)$, and the determinant of J is expressed by $M \equiv \det(J)$ as

$$M = -A - (2n+1)BX_k^{2n} - (4n+1)CX_k^{4n} - (6n+1)DX_k^{6n}. \quad (34)$$

We research equilibrium points that satisfy $X_\zeta = Y_\zeta = f(X) = 0$, and we find

$$\begin{cases} Y = 0, \\ X(A + BX^{2n} + CX^{4n} + DX^{6n}) = 0. \end{cases} \quad (35)$$

It is obvious to notice that $\text{Trace}(J) = 0$, and through the bifurcation theory [49, 50, 58], we know that, the solution (X_j, Y_j) of Eq. (35) is a:

- center point, if $M > 0$;
- saddle point, if $M < 0$;
- degenerate point, if $M = 0$.

From Eq. (35), firstly, we have one equilibrium point $(X, Y) = (0, 0)$ for the dynamical system Eq. (30), which is a center point, and hence stable.

- If we consider $A = 0$, we have

$$\begin{cases} Y = 0, \\ X^{2n+1}(B + CX^{2n} + DX^{4n}) = 0, \end{cases} \quad (36)$$

and by setting $\Delta = C^2 - 4BD$, we can discuss the following situations:

- If $\Delta < 0$, Eq. (36) has only one real root, which indicates that the dynamical system Eq. (30) has one equilibrium point $(X, Y) = (0, 0)$, which is a center point.
- If $\Delta = 0$ and $-\frac{C}{2D} > 0$, Eq. (36) has three real roots, which indicates that the dynamical system Eq. (30) has three equilibrium points: $(X, Y) \equiv (0, 0); \left(\sqrt[2n]{-\frac{C}{2D}}, 0\right); \left(-\sqrt[2n]{-\frac{C}{2D}}, 0\right)$. The first equilibrium point $(0, 0)$ is a center point; the second $\left(\sqrt[2n]{-\frac{C}{2D}}, 0\right)$ and third $\left(-\sqrt[2n]{-\frac{C}{2D}}, 0\right)$ points are also center points if $M > 0$. Else, if $M < 0$, they are saddle points and hence unstable.
- If $\Delta > 0$, $C < 0$, and $D < 0$, Eq. (36) has just one root; we find one equilibrium point $(0, 0)$, which indicates a stable center point.

- For $A \neq 0$, we get

$$\begin{cases} Y = 0, \\ A + BX^{2n} + CX^{4n} + DX^{6n} = 0. \end{cases} \quad (37)$$

We consider an evident root of the polynomial equation $A + BX^{2n} + CX^{4n} + DX^{6n} = 0$, as X_0 [i.e., $A + BX_0^{2n} + CX_0^{4n} + DX_0^{6n} = 0$] and setting $\Delta' = (C + DX_0^{2n})^2 - 4D[B + X_0^{2n}(C + DX_0^{2n})]$. After this consideration, we can discuss the equilibrium points for the dynamical system Eq. (30):

- If $\Delta' < 0$, we get a first equilibrium point as $(X_0, 0)$, which is a center point.
- If $\Delta' = 0$ and $-\frac{C+DX_0^{2n}}{2D} > 0$, there are three equilibrium points: one center point $(X_0, 0)$, and two saddle points $\left(\sqrt[2n]{-\frac{C+DX_0^{2n}}{2D}}, 0\right)$ and $\left(-\sqrt[2n]{-\frac{C+DX_0^{2n}}{2D}}, 0\right)$ for $M < 0$. In contrast for $M > 0$, the three equilibrium points are center points.
- If $\Delta' > 0$, $C > 0$, and $D > 0$, the dynamical system Eq. (30) has just equilibrium point $(X_0, 0)$, which indicates a stable center point.

Figure 3 shows the phase portrait of the dynamical system (30) for $a_1 = 1.4$, $a_2 = 1$, $b_1 = b_2 = \alpha = 2$, $\gamma = 3$, $\theta = 0.0005$, $\sigma = -4$, $k_1 = 0.51$, $k_2 = 3.5$, and $n = 1$. We observe one limit cycle about the origin $(0, 0)$. This implies that the waves are stable, and there are no noises to disturb them.

The periodicity of X and Y , based on system (30) with the same values of parameters as in **Figure 3**, is shown in **Figure 4**.

3.2.2 Quasiperiodic and chaotic motions of the perturbed system

In this section, we will study the quasiperiodic and chaotic motions for Eq. (1) under the external perturbation. As in the previous process, we find the following perturbed dynamical system:

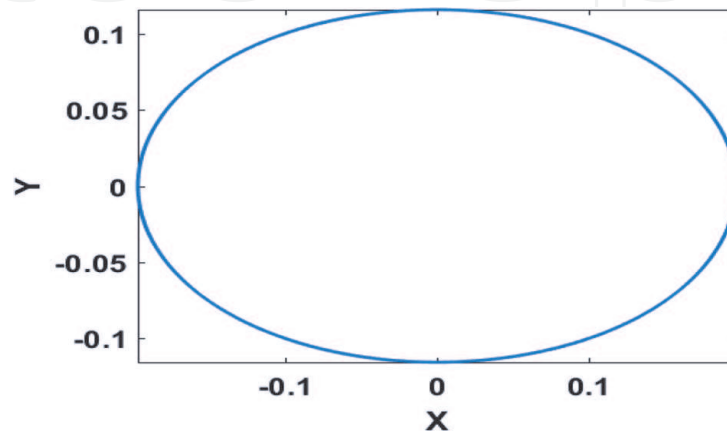


Figure 3. Phase portrait of the system (30) for parameter values: $a_1 = 1.4$, $a_2 = 1$, $b_1 = b_2 = \alpha = 2$, $\gamma = 3$, $\theta = 0.0005$, $\sigma = -4$, $k_1 = 0.51$, $k_2 = 3.5$, and $n = 1$.

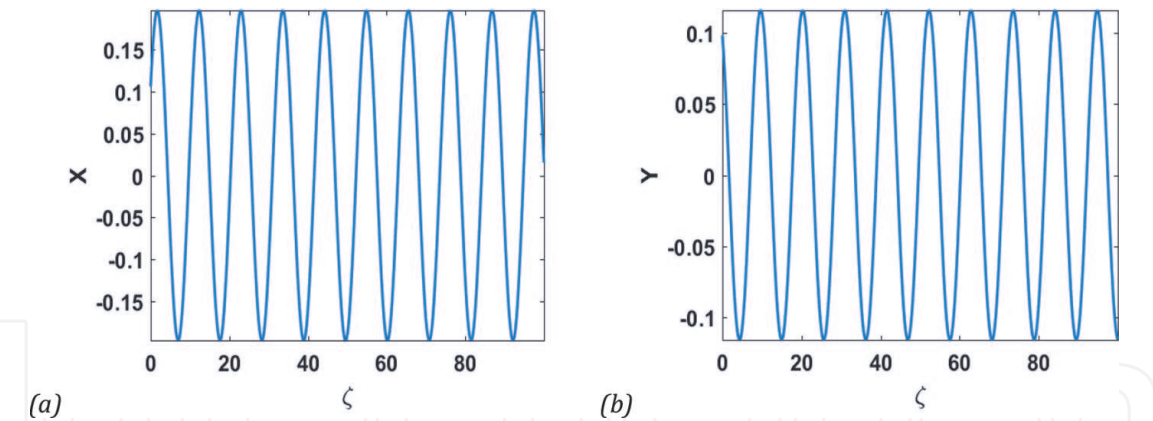


Figure 4. Periodicity of X and Y based on system Eq. (30), with the same values of parameters as **Figure 3**.

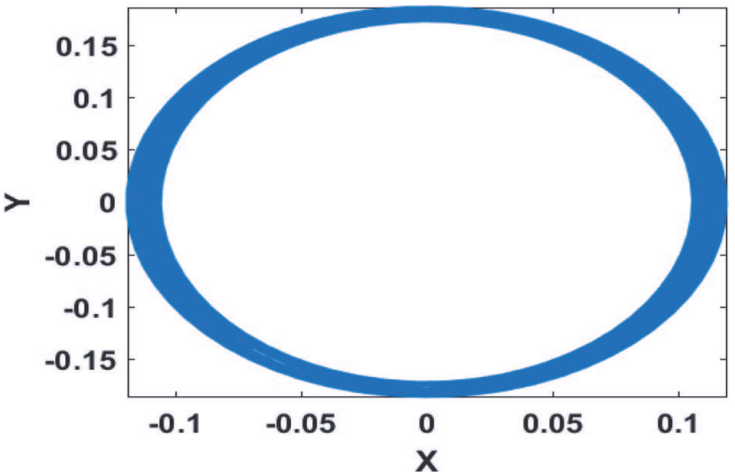


Figure 5. Phase portrait of the perturbed system (38) for the same parameter values as those in **Figure 3**, under external perturbation $R(\zeta) = E_0 \cos(\omega\zeta)$, where $E_0 = 0.01$ and $\omega = 1$.

$$\begin{cases} X_\zeta = Y, \\ Y_\zeta = g(X) = AX + BX^{2n+1} + CX^{4n+1} + DX^{6n+1} - \frac{R(\zeta)}{k_1(a_1k_1 - a_2k_2)}, \end{cases} \quad (38)$$

where X, Y, A, B, C , and D are given by Eqs. (28) and (29); $R(\zeta) = R_0 \cos(\omega\zeta)$ is an external periodic perturbation, R_0 is a strength of the external perturbation, and ω is the frequency. The difference between the system (30) and the system (38) is that only external periodic perturbation is added with the system (38).

In **Figure 5**, we have presented a phase portrait of the perturbed system (38) under the conditions of parameter values as those in **Figure 3**, except those fixed $E_0 = 0.01$ and $\omega = 1$. For the same parameter values as **Figure 5**, we plotted in **Figure 6** the quasiperiodicity of X and Y versus ζ . From this plot, it is obvious to notice that the perturbed system (38) has quasiperiodic motion even with the consideration of the external periodic perturbation.

If we increase the strength of the periodic perturbation by considering $E_0 = 0.01$, the other parameter values remain as in **Figure 5**, the perturbed system (38) shows quasiperiodic route to chaos as it is shown in **Figure 7**. In this case, the solutions ignore the periodic motions and represent random sequences of uncorrelated oscillations (see **Figures 7** and **8**).

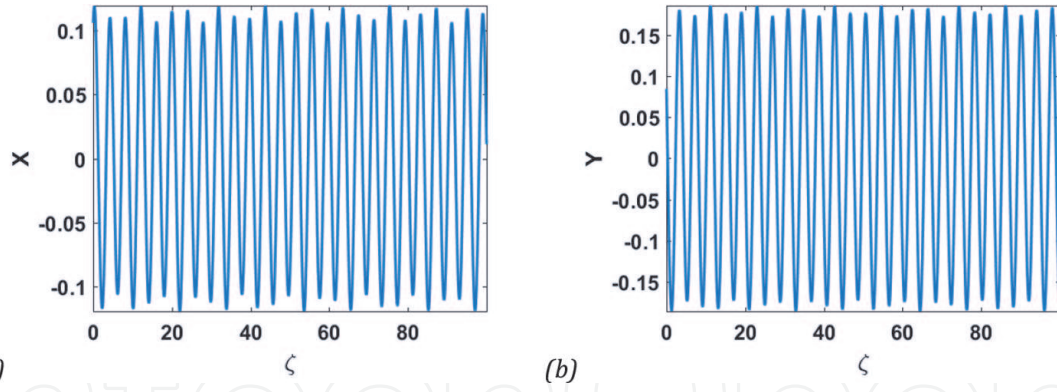


Figure 6. Variation of X and Y with respect to ζ of the perturbed system (38), for the same values of parameters as in Figure 5.

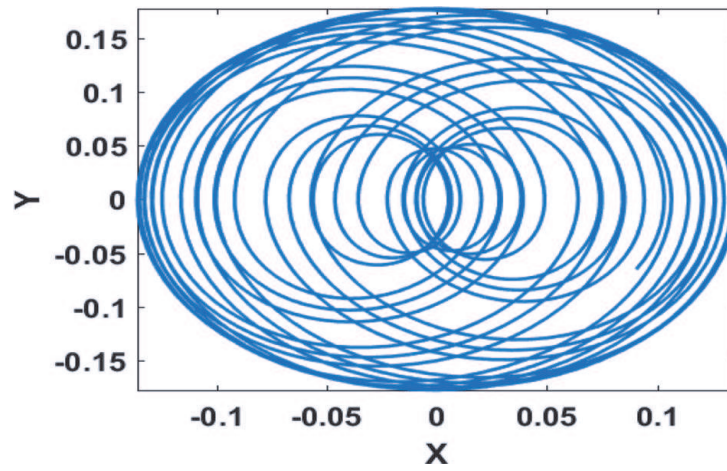


Figure 7. Phase portrait of the perturbed system (38) for the same parameter values as those in Figure 5 with $E_0 = 0.1$.

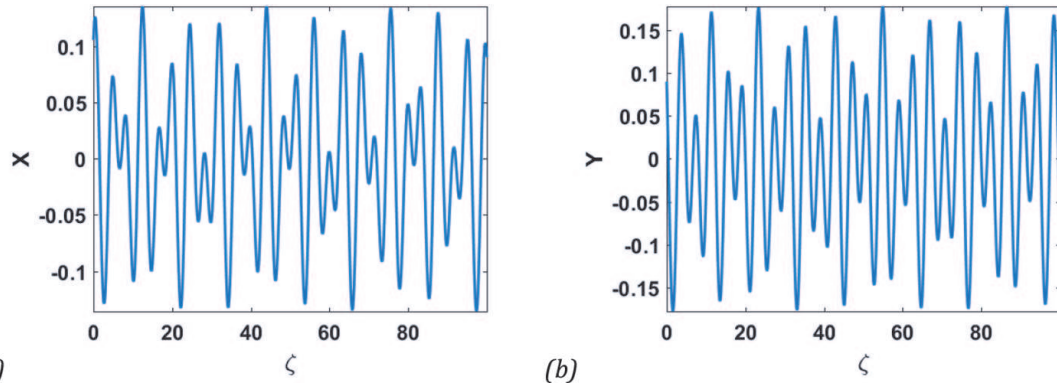


Figure 8. Quasi-periodicity of X and Y based on system (38), for same values of parameters as Figure 7.

From the above observations, it is straightforward to notice that the strength of the periodic perturbation significantly enhances the development of the quasiperiodic motion of the perturbed system (38) and quasiperiodic route to chaotic motion of the system (38). Thus, the perturbed NLS Eq. (1) with the power-law nonlinearity in a nano-optical fiber not only has solitonic and periodic wave solutions but could also possess quasiperiodic and chaotic motions.

4. Conclusion

In this chapter, we have investigated the perturbed nonlinear Schrodinger equation involving power-law nonlinearity and higher-order dispersions. We have constructed exact traveling wave solutions of the model by means of the well-known auxiliary equation method. We showed the existence of a family of traveling wave solutions and we have reported the parametric conditions on the physical parameters for the existence of these propagating solutions. Moreover, by employing Stuart and DiPrima's stability analysis method, a dispersion relation for the MI gain has been obtained. The outcomes of the instability development depend upon the nonlinearity, the power levels, and the dispersion parameters; the instability region increases regardless of the dispersion regime. The results may find straightforward applications in nonlinear optics, particularly in fiber-optical communication. Afterward, equivalent two-dimensional planar dynamic system and Hamiltonian have been derived and equilibrium points of the corresponding system have been gotten through the bifurcation theory. In addition, we have addressed the periodic, quasiperiodic, and chaotic behaviors of the traveling waves considering an external periodic perturbation. It has been observed that the perturbed system shows quasiperiodic route to chaos as a result of the strength of the periodic perturbation enhancement.

Conflict of interest

The authors declare no conflict of interest.

Appendix

The system of algebraic equations obtained by balancing $VV_{\zeta\zeta}$ and V^5 in Eq. (10) is as follows:

- V^5 coeff :

$$k_1(a_1k_1 - a_2k_2)(3n + 1)\mu_5 + 4n^2k_1p_2 = 0,$$

- V^4 coeff :

$$4n^2[b_2 + k_1p_1 + k_1p_2(\gamma + \theta) - p_2^2k_1(a_1k_1 - a_2k_2)] \\ + k_1(a_1k_1 - a_2k_2)(2n + 1)\mu_4 = 0,$$

- V^3 coeff :

$$4n^2[b_1 + k_1p_1(\gamma + \theta) + p_2(k_2 + \alpha k_1) - 2p_1p_2k_1(a_1k_1 - a_2k_2)] \\ + k_1(a_1k_1 - a_2k_2)(n + 1)\mu_3 = 0,$$

- V^2 coeff :

$$4n^2[p_1(k_2 + \alpha k_1) - p_1^2k_1(a_1k_1 - a_2k_2)] \\ + k_1(a_1k_1 - a_2k_2)\mu_2 = 0,$$

- V^1 coeff :

$$k_1(a_1k_1 - a_2k_2)(1 - n)\mu_1 = 0,$$

- V^0 coeff :

$$k_1(a_1k_1 - a_2k_2)(1 - 2n)\mu_0 = 0.$$

IntechOpen

Author details

Mati Youssoufa^{1*}, Ousmanou Dafounansou¹, Camus Gaston Latchio Tiofack²
and Alidou Mohamadou²

1 Faculty of Science, Department of Physics, University of Douala, Douala,
Cameroon

2 Faculty of Science, Department of Physics, University of Maroua, Maroua,
Cameroon

*Address all correspondence to: mati.youss@yahoo.fr

IntechOpen

© 2021 The Author(s). Licensee IntechOpen. This chapter is distributed under the terms of the Creative Commons Attribution License (<http://creativecommons.org/licenses/by/3.0>), which permits unrestricted use, distribution, and reproduction in any medium, provided the original work is properly cited. 

References

- [1] Schrödinger E. An undulatory theory of the mechanics of atoms and molecules. *Physical Review*. 1926;**28**: 1049-1070
- [2] Benney DJ, Newell AC. Nonlinear wave envelopes. *Journal of Mathematical Physics*. 1967;**46**:133-139
- [3] Zakharov VE. Stability of periodic waves of finite amplitude on the surface of a deep fluid. *Zhurnal Prikladnoj Mekhaniki i Tekhnicheskoy Fiziki*. 1968; **9**:86-94
- [4] Hasegawa A, Tappert FD. Transmission of stationary nonlinear optical pulses in dispersive dielectric fibers. I. Anomalous dispersion. *Applied Physics Letters*. 1973;**23**:142
- [5] Peregrine DH. Water waves, nonlinear Schrödinger equations and their solutions. *The Journal of the Australian Mathematical Society Series B Applied Mathematics*. 1983;**25**:16
- [6] Belmonte-Beitia J, Perez-Garcia VM, Vekslerchik V, Konotop VV. Localized nonlinear waves in systems with time- and space-modulated nonlinearities. *Physical Review Letters*. 2008;**100**: 164102
- [7] Chabchoub A, Hoffmann N, Onorato M, Slunyaev A, Sergeeva A, Pelinovsky E, et al. Observation of a hierarchy of up to fifth-order rogue waves in a water tank. *Physical Review E*. 2012;**86**:056601
- [8] Zhou Q, Liu L, Zhang H, Wei C, Lu J, Yu H, et al. Analytical study of Thirring optical solitons with parabolic law nonlinearity and spatio-temporal dispersion. *The European Physical Journal Plus*. 2015;**130**:138
- [9] Jiang Q, Su Y, Nie H, Ma Z, Li Y. New type gray spatial solitons in two-photon photorefractive media with both the linear and quadratic electro-optic effects. *Journal of Nonlinear Optical Physics & Materials*. 2017;**26**(1): 1750006
- [10] Topkara E, Milovic D, Sarma AK, Zerrad E, Biswas A. Optical solitons with non-Kerr law nonlinearity and inter-modal dispersion with time-dependent coefficients. *Communications in Nonlinear Science and Numerical Simulation*. 2010;**15**: 2320-2330
- [11] Jovanoski Z, Roland DR. Variational analysis of solitary waves in a homogeneous cubic-quintic nonlinear medium. *Journal of Modern Optics*. 2001;**48**:1179
- [12] Kivshar YS, Luther-Davies B. Dark optical solitons: Physics and applications. *Physics Reports*. 1998;**298**:81-197
- [13] Serkin VN, Belyaeva TL, Alexandrov IV, Melchior GM. Optical pulse and beam propagation III. In: Band YB, editor. *SPIE Proceedings*. Vol. 4271. Bellingham: SPIE; 2001. p. 292
- [14] Dai CQ, Wang YY, Zhang JF. Analytical spatiotemporal localizations for the generalized (3+1)-dimensional nonlinear Schrödinger equation. *Optics Letters*. 2010;**35**:1437
- [15] Jubgang D, Dikande AM, Sunda-Meya A. Elliptic solitons in optical fiber media. *Physical Review A*. 2015;**92**: 053850
- [16] Younis M, Rizvi S. Optical solitons for ultrashort pulses in nano fibers. *Journal of Nanoelectronics and Optoelectronics*. 2015;**10**:179
- [17] Tsaturian V, Sergeyev SV, Mou C, Rozhin A, Mikhailov V, Rabin B, et al. Polarisation dynamics of vector soliton molecules in mode locked fibre laser. *Scientific Reports*. 2013;**3**:3154

- [18] Herink G, Kurtz F, Jalali B, Solli DR, Ropers C. Real-time spectral interferometry probes the internal dynamics of femtosecond soliton molecules. *Science*. 2017;**356**:50
- [19] Chernysheva M, Bednyakova A, Araithi MA, Howe R, Hu G, Hasan T, et al. Double-wall carbon nanotube hybrid mode-locker in tm-doped fibre laser: A novel mechanism for robust bound-state solitons generation. *Scientific Reports*. 2017;**7**:44314
- [20] Yin HM, Tian B, Hu CC, Zhao XC. Chaotic motions for a perturbed nonlinear Schrödinger equation with the power-law nonlinearity in a nano optical fiber. *Applied Mathematics Letters*. 2019;**93**:139-146
- [21] Tahir M, Awan AU, Rehman HU. Dark and singular optical solitons to the Biswas-Arshed model with Kerr and power law nonlinearity. *Optik - International Journal for Light and Electron Optics*. 2019;**185**:777-783
- [22] Biswas A, Ekici M, Sonmezoglu A, Alqahtani RT. Sub-pico-second chirped optical solitons in mono-mode fibers with Kaup-Newell equation by extended trial function method. *Optik*. 2018;**168**: 208-216
- [23] Rogers C, Chow KW. Localized pulses for the quintic derivative nonlinear Schrödinger equation on a continuous-wave background. *Physical Review E*. 2012;**86**:037601
- [24] Yang B, Zhang W-G, Zhang H-Q, Pei S-B. Generalized Darboux transformation and rational soliton solutions for Chen–Lee–Liu equation. *Applied Mathematics and Computation*. 2014;**242**:863-876
- [25] Zhang J, Liu W, Qiu D, Zhang Y, Porsezian K, He J. Rogue wave solutions of a higher-order Chen–Lee–Liu equation. *Physica Scripta*. 2015;**90**: 055207
- [26] Bakodah H, Qarni AA, Banaja M, Zhou Q, Moshokoa SP, Biswas A. Bright and dark Thirring optical solitons with improved adomian decomposition method. *Optik*. 2017;**130**:1115-1123
- [27] Triki H, Babatin M, Biswas A. Chirped bright solitons for Chen–Lee–Liu equation in optical fibers and PCF. *Optik*. 2017;**149**:300-303
- [28] Arshad M, Seadawy A, Lu D, Wang J. Travelling wave solutions of Drinfel’d–Sokolov–Wilson, Whitham–Broer–Kaup and (2 + 1)-dimensional Broer–Kaup–Kupershmit equations and their applications. *Chinese Journal of Physics*. 2017;**55**:780-797
- [29] Banaja M, Qarni A, Bakodah H, Zhou Q, Moshokoa SP, Biswas A. The investigate of optical solitons in cascaded system by improved adomian decomposition scheme. *Optik*. 2017;**130**: 1107-1114
- [30] González-Gaxiola O, Biswas A. W-shaped optical solitons of Chen–Lee–Liu equation by Laplace–Adomian decomposition method. *Optical and Quantum Electronics*. 2018;**50**:314
- [31] Triki H, Zhou Q, Moshokoa SP, Ullah MZ, Biswas A, Belic M. Chirped wshaped optical solitons of Chen–Lee–Liu equation. *Optik*. 2018; **155**:208-12
- [32] Triki H, Hamaizi Y, Zhou Q, Biswas A, Ullah MZ, Moshokoa SP, et al. Chirped dark and gray solitons for Chen–Lee–Liu equation in optical fibers and PCF. *Optik*. 2018;**155**:329-33
- [33] Triki H, Hamaizi Y, Zhou Q, Biswas A, Ullah MZ, Moshokoa SP, et al. Chirped singular solitons for Chen–Lee–Liu equation in optical fibers and PCF. *Optik*. 2018;**157**:156-60
- [34] Kara A, Biswas A, Zhou Q, Moraru L, Moshokoa SP, Belic M. Conservation laws for optical solitons

with Chen–Lee–Liu equation. *Optik*. 2018;**174**:195-8

From Solitons to Similaritons. London: IntechOpen; 2020

[35] Youssoufa M, Dafounansou O, Mohamadou A. W-shaped, dark and grey solitary waves in the nonlinear Schrödinger equation competing dual power-law nonlinear terms and potentials modulated in time and space. *Journal of Modern Optics*. 2019;**66**(5): 530-540

[43] Hirota R. Exact envelope-soliton solutions of a nonlinear wave equation. *Journal of Mathematical Physics*. 1973; **14**:805-809

[36] Jawad AJAM, Biswas A, Zhou Q, Alfiras M, Moshokoa SP, Belic M. Chirped singular and combo optical solitons for Chen–Lee–Liu equation with three forms of integration architecture. *Optik*. 2019;**178**:172-7

[44] Sasa N, Satsuma J. New-type of soliton solutions for a higher-order nonlinear Schrödinger equation. *Journal of the Physical Society of Japan*. 1991; **60**:409-9

[37] Kudryashov NA. General solution of the traveling wave reduction for the perturbed Chen–Lee–Liu equation. *Optik*. 2019;**186**:339-49

[45] Savescu M, Khan KR, Kohl RW, Moraru L, Yildirim Y, Biswas A. Wavelength selective supercontinuum signal generated from photonic crystal fibers for microscopic object detection. *Journal of Nanoelectronics and Optoelectronics*. 2013;**8**:208

[38] Xie XY, Meng GQ. Dark solitons for the $(2+1)$ -dimensional Davey–Stewartson-like equations in the electrostatic wave packets. *Nonlinear Dynamics*. 2018;**93**:779

[46] Mirzazadeh M, Ekici M, Sonomezoglu A, Eslami M, Zhou Q, Kara AH, et al. Optical solitons with complex Ginzburg–Landau equation. *Nonlinear Dynamics*. 2016;**5**(3): 1979-2016

[39] Mohammed ASHF, Bakodah HO, Banaja MA. Approximate Adomian solutions to the bright optical solitary waves of the Chen–Lee–Liu equation. *MATTER: International Journal of Science and Technology*. 2019;**5**:110-20

[47] Biswas A, Yildirim Y, Yasar E, Triki H, Alshomrani AS, Ullah MZ, et al. Optical soliton perturbation with complex Ginzburg–Landau equation using trial solution approach. *Optik*. 2018;**160**:44-60

[40] Ahmed I, Seadawy AR, Lu D. M-shaped rational solitons and their interaction with kink waves in the Fokas–Lenells equation. *Physica Scripta*. 2019;**94**:055205

[48] Abdoukary S, Mohamadou A, Beda T, Gambo B, Doka SY, Alim, Mahamoudou A. Exact traveling wave solutions to the nonlinear Schrödinger equation. *Applied Mathematics and Computation*. 2014;**233**:109-115

[41] Arshad M, Lu D, Rehman M-U, Ahmed I, Sultan AM. Optical solitary wave and elliptic function solutions of the Fokas–Lenells equation in the presence of perturbation terms and its modulation instability. *Physica Scripta*. 2019;**94**:105202

[49] Saha A. Bifurcation of travelling wave solutions for the generalized KP-MEW equations. *Communications in Nonlinear Science and Numerical Simulation*. 2012;**17**:3539

[42] Youssoufa M, Dafounansou O, Mohamadou A. *Nonlinear Optics –*

[50] Guckenheimer J, Holmes PJ. *Nonlinear Oscillations, Dynamical Systems and Bifurcations of Vector Fields*. New York: Springer-Verlag; 1983

[51] Gradshteyn IS, Ryzhik IM. Table of Integrals, Series, and Products. 7th ed. London: Academic Press; 2007

[52] Agrawal GP. Nonlinear Fiber Optics. New York: Academic Press; 2013

[53] Kivshar YS, Agrawal GP. Optical Solitons: From Fibers to Photonic Crystal. San Diego: Academic Press; 2003

[54] Shukla PK, Rasmussen JJ. Modulational instability of short pulses in long optical fibers. Optics Letters. 1986;**11**:171

[55] Potasek MJ. Modulation instability in an extended nonlinear Schrödinger equation. Optics Letters. 1987;**12**:921

[56] Mohamadou A, Latchio Tiofack CG, Kofané TC. Wave train generation of solitons in systems with higher-order nonlinearities. Physical Review E. 2010; **82**:016601

[57] Porsezian K, Nithyanandan K, Vasantha Jayakantha Raja R, Shukla PK. Modulational instability at the proximity of zero dispersion wavelength in the relaxing saturable nonlinear system. Journal of the Optical Society of America. 2012;**B29**:2803

[58] Infeld E, Rowlands G. Nonlinear Waves, Solitons and Chaos. Cambridge: Cambridge University Press; 1990